Reflectivity and Attenuation at Millimeter to Infrared Wavelengths for Advection Fogs at Four Locations

DAVID A. DE WOLF AND CHRISTOS KONTOGEORGAKIS

Bradley Department of Electrical Engineering, Virginia Polytechnic Institute and State University, Blacksburg, Virginia

ROBERT E. MARSHALL

Department of Civil Engineering, Virginia Polytechnic Institute and State University, Blacksburg, Virginia

(Manuscript received 5 September 1997, in final form 13 April 1998)

ABSTRACT

Recent drop size distribution data from four advection fog sites are reanalyzed for the purpose of predicting millimeter-wave and infrared to visible wavelength reflectivity and attenuation coefficients in such fogs. A gamma drop size distribution model is shown to be an adequate fit to measured distributions of typical fog drop diameters. Conclusions are drawn with respect to the relationships between the reflectivity and the attenuation to the liquid water content. A possible method is outlined for using ground-based measurement of liquid water content for the purpose of predicting arbitrary slant-path reflectivity and attenuation at the smaller wavelengths.

1. Introduction

This work reexamines the inference of millimeter-wave and optical attenuation in—and reflection from—fogs and/or hazes in the light of relatively new and interesting data (Zak 1994) on the distribution of drop sizes in four advection fogs in the first few hundred meters above the ground. The wavelengths of interest lie in the 35–95-GHz radar regime (2–8 mm) and in the infrared to visible regime (0.4–12 μm). Knowledge of reflectivity and attenuation is of special importance for evaluating the visibility in situations in which aircraft are involved. The theoretical background linking electromagnetic (EM) to meteorological parameters seems to be well understood in general (Doviak and Zrnic 1993), and there are abundant empirical relationships (Atlas 1964) that relate reflectivity, attenuation, and liquid water content to each other and to relevant parameters of the medium and measuring instruments. The ability to measure drop sizes reasonably accurately has also made it possible to discriminate between some of the various empirical relationships and to provide a theoretical basis. However, the wavelengths in question approach and become as small as (if not smaller than) the drop sizes, resulting in some of the customarily used relationships becoming invalid because they are based on the Rayleigh-regime approximations (drop size $\ll$ wavelength). The data analyzed in this work provide an opportunity to predict what radars and optical instruments might observe.

Several findings can be summarized as follows. First, we found that the distribution of drops with diameter D, namely, $n_4(D, z)$ [in m^{-4}], can be fitted with a gamma distribution $\alpha(z)D^4 \exp(-D/D_o)$ in which the parameter D_o appears to be a weak function of location and almost not at all of altitude z. Second, we have found, at least in the advection fogs, that the Rayleigh-regime reflectivity coefficient $Z(z)$ is closer to being a linear function of the liquid water content $M(z)$ rather than a quadratic one, as predicted by Atlas (1964) for clouds. Third, we have found that the ratio between the reflectivity and the attenuation coefficient to $M(z)$ is a function of wavelength that varies weakly from location to location for the infrared-to-visible wavelength regimes.

2. Brief summary of the experiment

The drop size data upon which this work is based (Zak 1994) were obtained during flight tests involving descents along a 3° glide slope in which onboard instrumentation measured the number of drops in ''bins'' of 3-μm spreads in drop diameter up to a diameter of 47 μm using a Particle Systems, Inc., forward scattering spectrometer probe (FSSP-100) mounted on a wing (Dye and Baumgartner 1984; additional information available from Web site raf.atd.ucar.edu/~darrell/htmFiles/fssp100.html and raf.atd.ucar.edu/~darrell/

Corresponding author address: David A. de Wolf, Bradley Department of Electrical Engineering, 340 Whittemore Hall, Virginia Tech, Blacksburg, VA 24061-0111.
E-mail: dadewolf@vt.edu

htmFiles/260X.html). These descents were part of a Federal Aviation Administration program to test the capability of millimeter-wave radar and infrared cameras to provide a runway image in the cockpit of aircraft attempting landings in fog. Larger drops were noted in 20- and 300-μm bins by means of an optical array probe (OAP 200X or 200Y) mounted on the other wing (Baumgardner and Korolev 1997), but there is uncertainty as to what extent the noted effect upon drop size distribution of these larger particles will really be in fog. The flights occurred at four distinct advection fog sites: Vandenberg AFB; California (VAN); Worcester, Massachusetts (WOR); Arcata, California (ARC); and Santa Maria, California (SM). The VAN and ARC sites are directly adjacent to the Pacific Ocean. Measurements at VAN on 27 August 1992 and at ARC on 28 August 1992 were on similar ocean-produced fogs moving inland at surface wind speeds of less than 3 m s^{-1}. Some drizzle was reported. The SM site is 18 km farther inland. The SM measurements of 23 September 1992 dealt with a fog that was nearing a dissipation stage more than the others, but there was no rain. The WOR site is 73 km west-southwest (WSW) of Boston's Logan Airport, and measurements there on 26 September 1992 concerned remains of Tropical Storm Danielle moving northeast at a speed of 4–5 m s^{-1}, leading to fog and rain locally with drizzle during some of the airplane approaches during fog conditions.

3. Basic formulation

The following very brief summary of the relationships between EM and meteorological parameters should suffice as a background. The radar backscatter cross section per unit volume of spherical scatterers, Q (in m^2 m^{-3}), expresses the ratio of reflected plane-wave flux to incident spherical electromagnetic power flux in terms of an equivalent area per unit volume:

$$Q = 4\pi \exp\left[-2\int^{z} d\zeta\gamma(\zeta)\right]\int dDn_4(D,z)\sigma_{\rm bs}(\lambda, D, \varepsilon), \tag{1}$$

where $\sigma_{\rm bs}(\lambda, D, \varepsilon)$ is the backscatter power attenuation coefficient (Bohren and Huffman 1983) for a single particle, as described by the Mie theory (Mie 1908) for a spherical particle, and $\int^{z} d\zeta\gamma(\zeta)$ is the one-way path integral of the attenuation coefficient $\gamma(\zeta)$ between the power source and the unit volume. The radar/laser wavelength and particle permittivity are given, respectively, by λ and ε. Formulation in terms of the Mie theory is increasingly important as radar wavelengths move into the millimeter regime. The attenuation coefficient at altitude z is given (van de Hulst 1957) by

$$\gamma(z) = \frac{2\lambda}{\sin\theta}\int dDn_4(D, z)Im[f_{\rm fs}(\lambda, D, \varepsilon)], \tag{2}$$

for a glide slope at elevation angle θ with single-particle forward scattering amplitude $f_{\rm fs}(\lambda, D, \varepsilon)$. The liquid water content of a unit volume of droplets at altitude z is given by,

$$M(z) = \frac{\pi}{6}\rho_w\int dDD^3n_4(D, z), \tag{3}$$

where ρ_w is the specific mass of water, for example, in g m^{-3}. Equations (1)–(3) are well known and are cited in many places. In the Rayleigh regime of very small particles ($D \ll \lambda$), it follows (van de Hulst 1957; Kerr 1965) that

$$f_{\rm fs}(\lambda, D, \varepsilon) = f_{\rm bs}(\lambda, D, \varepsilon) = \frac{\pi^2D^3}{2\lambda^2}\frac{\varepsilon - 1}{\varepsilon + 2}, \tag{4}$$

where $\sigma_{\rm bs}(\lambda, D, \varepsilon) = |f_{\rm bs}(\lambda, D, \varepsilon)|^2$ so that (1) becomes

$$Q(z) = \exp\left[-2\int^{z} d\zeta\gamma(\zeta)\right]\frac{\pi^5}{\lambda_4}\left|\frac{\varepsilon - 1}{\varepsilon + 2}\right|^2 Z(z),$$

$$Z(z) = \int dDD^6n_4(D, z), \tag{5}$$

in what is known as the Rayleigh regime of scattering. Here, $Z(z)$ is known as the reflectivity factor, and it is purely a function of the drop size distribution. Alternative expressions for $Z(z)$ specifically in the Rayleigh regime and for $M(z)$ in general are,

$$Z(z) = \left(\frac{6}{\pi}\right)^2 n_3(z)\langle v^2(z)\rangle \quad \text{and} \quad M(z) = \rho_w n_3(z)\langle v(z)\rangle, \tag{6}$$

where $n_3(z)$ is the particle density (in m^{-3}), and $\langle v^n(z)\rangle$ is the nth moment of the particle volume $\pi D^3/6$ [i.e., the sum of all particle volumes per unit volume weighted by $n_4(D, z)$ and divided by $n_3(z)$]. Similar formulas can be found, among others, in Paluch et al. (1996). From (6), it follows that

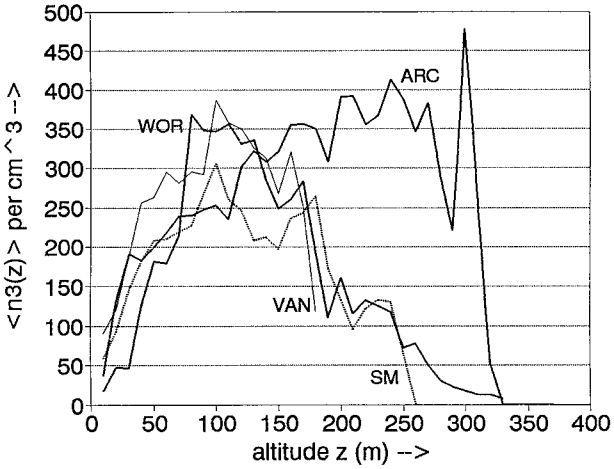

FIG. 1. Averaged particle densities $n_3(z)$ as functions of altitude z for the four sites.

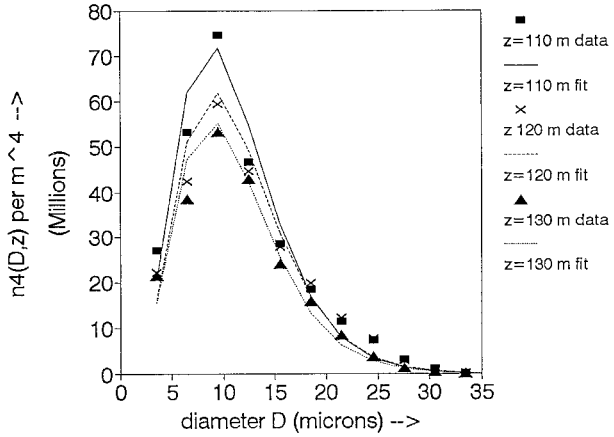

FIG. 2. Sample-averaged drop size distributions at three altitudes for site VAN and fits by gamma drop size distributions $\propto D \exp(-D/D_o)$.

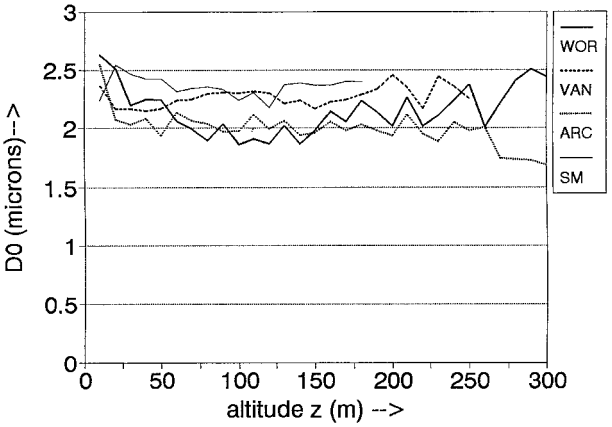

FIG. 3. Gamma function exponential parameter D_o vs altitude z for the four sites.

$$Z(z) = \left(\frac{6}{\pi}\right)^2 \frac{\langle v^2(z)\rangle}{\langle v(z)\rangle} \frac{1}{\rho_w} M(z). \tag{7}$$

This can express a linear relationship between M and Z, provided $\langle v^2(z)\rangle/\langle v(z)\rangle$ is not a function of altitude. For the above-mentioned gamma distribution model, $n_4(D, z) = \alpha(z)D^4 \exp(-D/D_o)$ as well as for many other commonly used analytical models (Deepak 1982), it is easily seen that $\langle v^m(z)\rangle$ is not a function of altitude z, so that the coefficient of $Z(z)/M(z)$ is not altitude dependent (as long as D_o also is not a function of z). However, nonlinear relationships between M and Z can result when the measured quantities underlying the calculations are averaged differently (see below).

4. The particle drop size data

The data (Zak 1994) consist largely of number densities for particles with diameters D in 3-μm ''bins'' such that $d - 1.5 < (D \text{ in } \mu\text{m}) < d + 1.5$ in a bin, with $d = 3.5, 6.5, \ldots, 45.5$ μm. The particle diameters thus lie between 2 and 47 μm. The data were gathered every 10 m of altitude from about 400 m altitude down. Two problems were encountered: 1) 2 to 10 runs were conducted for each fog so that the sampling varied highly and 2) the instrumentation was not able to register densities below 10^4 m^{-3} per bin, so that false zeros were registered where there may have been lower densities. Figure 1 shows cumulative densities $n_3(z)$ obtained at each altitude and site from the raw data by averaging over the runs. Not shown but implicit are fairly large standard deviations of up to 50% or so around these averages (which reflect changing weather conditions from run to run). The small-scale irregularities in these data also are partly due to the false zeros registered for low density values.

Figure 2 shows VAN raw-data curves of $n_4(D, z)$ as a function of particle diameter D for several altitudes z. These are compared to gamma distribution curves obeying

$$n_4(D, z) = \alpha(z)D^4 e^{-D/D_o}, \tag{8}$$

which are fitted to the data curves by minimizing the least square residuals. These also are shown in the figure. We have found that a factor D^4 fits well with a value of D_o that is not dependent upon altitude. However, the raw-data curves at altitude extremes (where particle densities are lower) tend more to resemble Junge distributions (Deepak 1982). Table 1 gives best-fit values of $\alpha(z)$ and D_o for these data. The standard deviations in D_o indicate relatively small variations with altitude. Figure 3 shows values of D_o versus altitude z for the four advection fog sites. Deviations from a constant value occur at altitudes where either data are sparse or densities are close to threshold measurement values. The modeled distribution may not be unique for these data, but it is adequate.

The liquid water content $M(z)$, as defined by (3), is determined by the particle drop size distribution. It is obvious from use of (8) in $\langle v^n(z)\rangle$ that both $\langle v(z)\rangle$ and $\langle v^2(z)\rangle$ are independent of altitude and that therefore the

TABLE 1. Parameters for gamma drop size distribution $n_4(D, z)$.

	$\alpha(z)$ (μm^{-4} m^{-4})	D_o (μm)	Range of z (m)
VAN	$79\,233 + 1675.6z - 6.538z^2$	2.27 ± 0.09	$0 < z < 297$
WOR	$0.177z^{4.125}e^{-0.0396z}$	2.10 ± 0.09	$0 < z < 390$
ARC	$-2962 + 8877z - 83.7z^2 + 0.374z^3 - 0.000578z^4$	1.96 ± 0.08	$0.3 < z < 365$
SM	$2271z + 16.49z^2 - 0.1523z^3$	2.36 ± 0.035	$0 < z < 188$

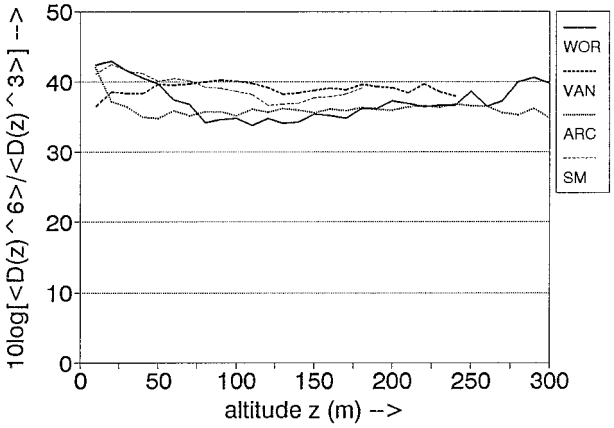

FIG. 4. Test of volume moments ratio $\langle v^2(z)\rangle/\langle v(z)\rangle$ vs altitude z for the four sites.

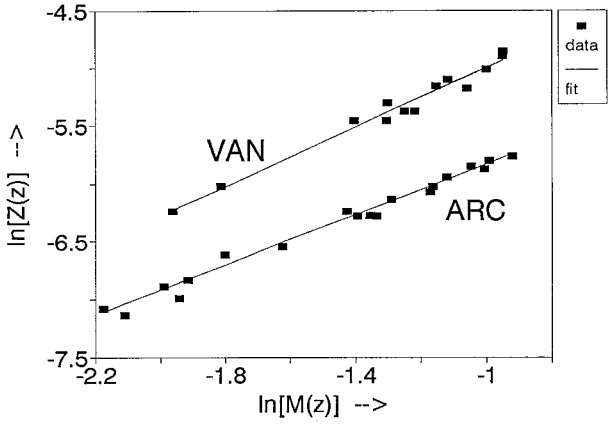

FIG. 5. Plots of reflectivity factor $\ln[Z(z)]$ vs liquid water content $\ln[M(z)]$ to test for power law.

ratio of $Z(z)$ to $M(z)$ is independent of altitude z when both of these quantities are computed with the model (8). To test whether this is really the case for the actual data at these sites, we have calculated $\langle v^2(z)\rangle/\langle v(z)\rangle$ using the averaged $n_4(D, z)$ data at each site rather than the model (8). Figure 4 shows equivalent graphs of 10 $\log_{10}[\langle D^6(z)\rangle/\langle D^3(z)\rangle]$ versus z for each of the advection fog sites. This ratio at WOR is 35.9 ± 1.28 dB in the regions of significant measurements; the standard deviations are smaller for VAN and ARC and only slightly larger for SM. It seems reasonable to expect little variation of Z/M with altitude.

5. The relationship between $Z(z)$ and $M(z)$

The constancy with altitude of $\langle v^2(z)\rangle/\langle v(z)\rangle$ suggests [see (7)] that the reflectivity factor $Z(z)$ is a linear function of liquid water content $M(z)$ for these data at low frequencies. The quadratic relationship (Atlas 1964) for uniform size droplets in clouds would not be valid here. That different power laws are measured seems often to be a function of what is averaged. If, for instance, the data for both quantities are averaged at a fixed altitude, $z = 150$ m, over the four sites, then the relationship (Z in mm^6 m^{-3}) ≈ 0.0251 (M in g m^{-3})$^{1.583}$ is found from the model. Figure 5 shows an evaluation of $\ln[\overline{Z}(z)]$ versus $\ln[\overline{M}(z)]$ for the VAN site at significant altitudes $40 \le (z \text{ in m}) \le 150$, and for the ARC site at $60 < (z \text{ in m}) < 240$, for the actual averaged $n_4(D, z)$ data. The overbar indicates averaging at fixed altitude over a number of runs. Regression analysis yields

$$(\overline{Z} \text{ in mm}^6 \text{ m}^{-3}) = (0.0244 \pm 0.0015)(\overline{M} \text{ in g m}^{-3})^{(1.282)}, \quad \text{VAN site,}$$

and

$$(\overline{Z} \text{ in mm}^6 \text{ m}^{-3}) = (0.00882 \pm 0.00029)(\overline{M} \text{ in g m}^{-3})^{(1.106)}, \quad \text{ARC site.} \tag{9a}$$

Only these two sites had enough data runs so that averages of the $n_4(D, z)$ values would overcome the low-threshold limitations sufficiently. In checking the linear relationship for these same data we find for the ratio $\overline{Z}(z)/\overline{M}(z)$:

$$(\overline{Z}/\overline{M} \text{ in mm}^6 \text{ g}^{-1}) = (0.0172 \pm 0.0018), \quad \text{VAN site}$$
$$(\overline{Z}/\overline{M} \text{ in mm}^6 \text{ g}^{-1}) = (0.00758 \pm 0.00050), \quad \text{ARC site.} \tag{9b}$$

It is difficult to discriminate between (9a) and (9b) for these data as the errors in $\overline{Z}/\overline{M}$, $\overline{Z}/\overline{M}^{1.282}$ and $\overline{Z}/\overline{M}^{1.106}$ are similar.[1] Furthermore, radar or optical measurements take into account the nonzero drop concentrations that the VAN, etc., measurements were not able to see. For these reasons. it is not straightforward to predict a unique Z versus M relationship that holds for EM reflectivity under the conditions of these measurements.

At infrared to visible wavelengths, the second relationship in (5) is no longer valid. In that case, one needs to work with

$$Z(z) = \exp\left[2\int^z d\zeta\gamma(\zeta)\right]\frac{\lambda^4}{\pi^5}\left|\frac{\varepsilon + 2}{\varepsilon - 1}\right|^2 Q(z), \tag{10}$$

where $Q(z)$ is given by (1). Using the model (8) and Mie theory for the scattering amplitudes in (1), and then substituting the result for zero attenuation into (10), we obtain a linear relationship between $Z(z)$ and $M(z)$, the ratio of which is a function of wavelength λ (but not of z), as shown in Fig. 6. The data in Fig. 6, sampled at frequencies, each of which is a factor 1.02 larger than the previous one, appear to show most of the salient

[1] The power-law dependence also can be explained by the possibility that parameter D_o is dependent upon altitude. In that case the form (8) of the drop size distribution yields $Z(z) \propto M(z)^{(4+6+1)/(4+3+1)}$ or $Z(z) \propto M(z)^{11/8}$. We are indebted to a referee for pointing out this possibility.

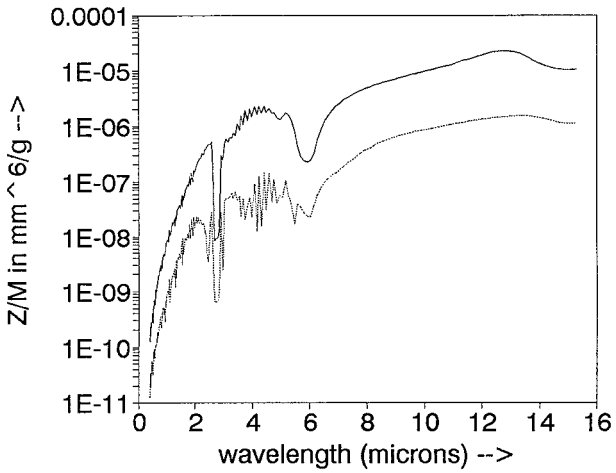

FIG. 6. The reflectivity factor to liquid water content ratio Z/M vs wavelength. The solid line denotes the average ratio and the dotted line denotes the standard deviation of the ratio.

features, and the relatively small standard deviation curve indicates that one average curve is useful for all four sites at infrared to visible wavelengths. The apparent universality of this curve is largely determined

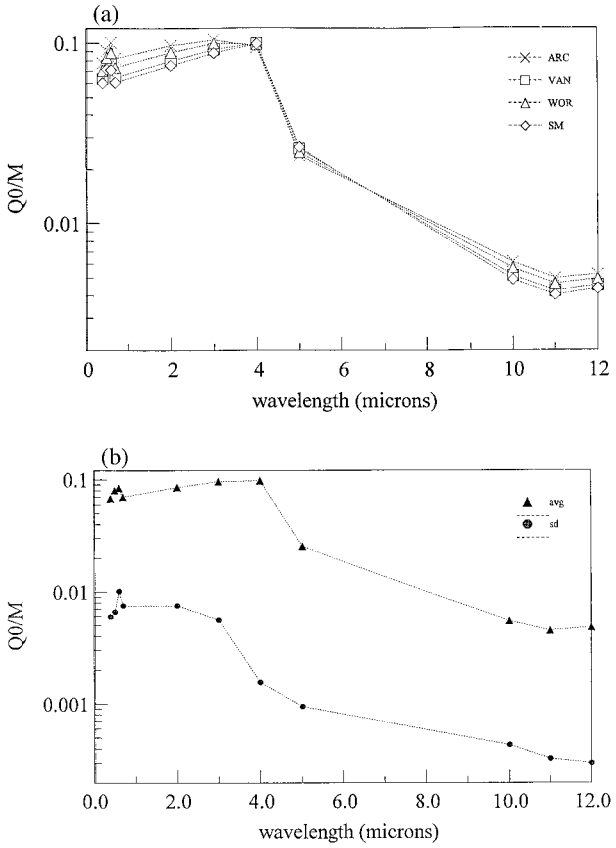

FIG. 7. (a) The backscatter cross section to liquid water content ratio Q_o/M vs wavelength for 11 selected wavelengths at four sites. (b) Average and standard deviation of the four Q_o/M curves of (a).

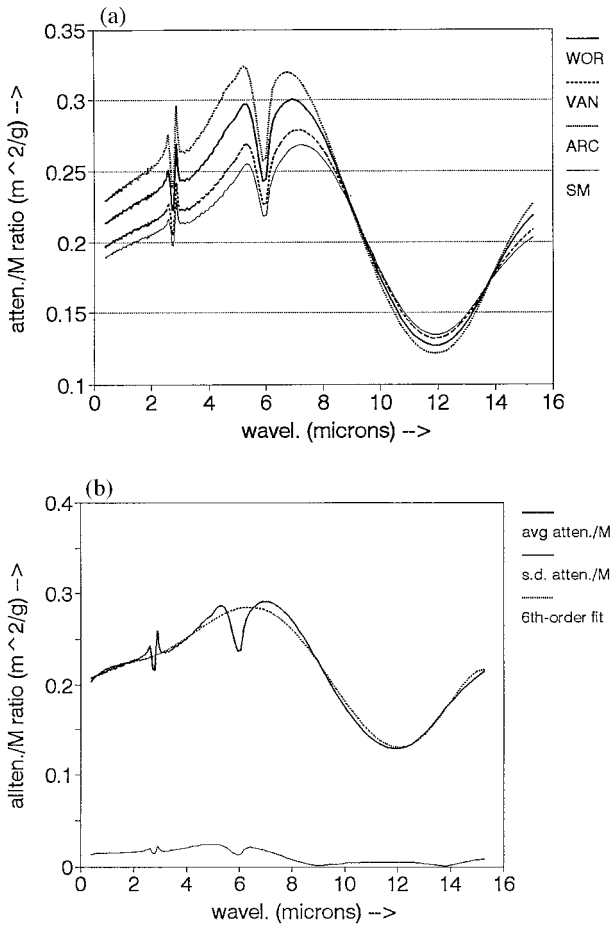

FIG. 8. (a) The attenuation coefficient to liquid water content ratio γ/M vs wavelength for the infrared to visible wavelength regime at four sites. (b) Average and standard deviation of the four γ/M curves of (a).

by $\sigma_{bs}(\lambda, D, \varepsilon)$, as can be understood from (1). A relationship between the zero-attenuation cross section $\eta(z) \equiv Q_o(z)$ and $M(z)$ follows from this curve and from

$$Q_o(z) = \frac{\pi^5}{\lambda^4}\left|\frac{\varepsilon - 1}{\varepsilon + 2}\right|^2 Z(z). \tag{11}$$

The ratio Q_o/M is shown as a function of wavelength in the infrared to visible regime in Fig. 7a for all four sites, and the average and standard deviation are depicted for 11 representative frequencies in Fig. 7b. To obtain the cross section $Q(z)$ with the exponential attenuation factor in (5), the relationship between $\gamma(z)$ and $M(z)$ is required. Using (2), the ratio $\gamma(z)/M(z)$ is shown as a continuous function of wavelength in the infrared to visible regime in Fig. 8a, for all four sites, and the average and standard deviation are depicted in Fig. 8b. Figure 8b also shows a sixth-order polynomial fit to the average $\gamma(z)/M(z)$ versus λ curve.

From these observations, it seems possible to deduce attenuation and reflection coefficients in the infrared to

visible regime from knowledge of the liquid water content $M(z)$. Both $Q_o(z)/M(z)$ and $\gamma(z)/M(z)$ then appear to be predictable at these frequencies from single curves of each ratio versus wavelength λ, from which we also can construct $Q(z)$ as well as the attenuation $\int dz\ \gamma(z)$.

6. Prediction of $M(z)$ required for reflectivity and attenuation

Here, we will describe briefly a possible method for predicting infrared and visible attenuation that an airplane preparing to land in fogs (of the type discussed) would encounter. The method rests on the assumption that a millimeter-wave radar is available at the landing site to probe the fog. We assume that the radar can measure accurately, at millimeter wavelength, the radar cross section of a known object (e.g., a sphere of known radius rising by means of a balloon through the fog). Assume that the radar cross section of the object in free space would be Q_{obj}. The actually measured cross section of the object, with known radar cross section Q_{obj}, rising in a fog would be

$$Q_{\text{meas}}(z) = \exp\left[-2\int^{z} d\ell\,\gamma(z)\right]Q_{\text{obj}}, \qquad \ell = z/\sin\theta, \tag{12}$$

if θ is the elevation angle, and with $\gamma(z)$ given by the Rayleigh-regime formula,

$$\gamma(z) = \frac{6\pi}{\lambda\rho_w}\text{Im}\left(\frac{\varepsilon - 1}{\varepsilon + 2}\right)M(z). \tag{13}$$

From these formulas, it follows that

$$d\,\ln[Q_{\text{meas}}(z)]/dz = -2\frac{\gamma(z)}{\sin\theta} = \frac{-12\pi}{\lambda\rho_w\sin\theta}\text{Im}\left(\frac{\varepsilon-1}{\varepsilon+2}\right)M(z), \tag{14}$$

from which we obtain, by inversion, the liquid water content $M(z)$. The above curves of γ/M and Q/M then predict attenuation and reflectivity at infrared to visible frequencies.

7. Final comments

We have noted that several of the sites measured a number of drops with diameters larger than 50 μm. For example, the VAN and ARC data shows some runs in which drops with diameters up to 270 μm (partially if not wholly due to drizzle) were noted. An analysis shows that these sparsely distributed large drops do not significantly affect our estimates of $M(z)$, nor of $\gamma(z)$, but they do significantly change the estimates of $Z(z)$, given as a sum or integral of $D^6 n_4(D, z)$, due to the strong effect of the sixth power of diameter D. However, the particle backscatter amplitudes, $f_{\text{bs}}(\lambda, D, z)$, at infrared to visible wavelengths are much lower than would be predicted from (4) at the same wavelengths. Nevertheless, an exploratory analysis of the effect of these large particles does indicate an appreciable effect upon $Q(z)$—of the order of an extra 10 dB at $\lambda = 3$ μm for VAN. A gamma distribution of $n_4(D, z)$ does not seem feasible for the large-drop tails, as these do not decrease sufficiently rapidly with increasing D. Nevertheless, modeling similar to the above can be done with inclusion of the larger particles. The above analysis has not included the effect of these drops because 1) not all sites exhibited appreciable numbers of large drops, 2) there are greater inaccuracies in the large-particle measurements by FSSP (Paluch et al. 1996), and 3) advection fogs normally do not have drops much larger than $D =$ 50 μm; the larger drops may have been due to drizzle. The effect of large drops upon attenuation is expected to be considerably smaller, for example, because that quantity depends on an integral of approximately $D^3 n_4(D, z)dD$, as opposed to a D^6 factor. In fact, a check shows the effect to be less than 10%.

REFERENCES

Atlas, D., 1964: Advances in radar meteorology. *Advances in Geophysics*, Vol. 10, Academic Press, 317–479.

Baumgardner, D., and A. V. Korolev, 1997: Air speed corrections for optical array probes. *J. Atmos. Oceanic Technol.*, **14,** 1224–1229.

Bohren, C. F., and D. R. Huffman, 1983: *Absorption and Scattering of Light by Small Particles.* Wiley and Sons, 530 pp.

Deepak, A., 1982: *Atmospheric Aerosols.* Spectrum, 480 pp.

Doviak, R. J., and D. S. Zrnic, 1993: *Doppler Radar and Weather Observations.* 2d ed. Academic Press, 562 pp.

Dye, J. E., and D. Baumgardner, 1984: Evaluation of the forward scattering spectrometer probe. Part I: Electronic and optical studies. *J. Atmos. Oceanic Technol.,* **1,** 329–344.

Kerr, D. E., 1965: *Propagation of Short Radio Waves.* Dover, 727 pp.

Mie, G., 1908: Beitrage zur Optik trüber Medien speziell kollidaler Metallösungen. *Ann. Phys.,* **25,** 377–445.

Paluch, I. R., C. A. Knight, and L. J. Miller, 1996: Cloud liquid water and radar reflectivity of nonprecipitating cumulus clouds. *J. Atmos. Sci.,* **53,** 1587–1603.

van de Hulst, H. A., 1957: *Light Scattering by Small Particles.* Wiley and Sons, 470 pp.

Zak, J. A., 1994: Drop size distributions and related properties of fog for five locations measured from aircraft. NASA Contractor Rep. 4585, 129 pp. [Available from NASA Langley Research Center, Hampton, VA 23681-0001.]